Open Archive Toulouse Archive Ouverte (OATAO)

OATAO is an open access repository that collects the work of some Toulouse researchers and makes it freely available over the web where possible.

This is an author's   version published in: https://oatao.univ-toulouse.fr/22908

Official URL : http://dx.doi.org/10.1063/1.4900465

To cite this version :

Rizzolo, Serena and Morana, Adriana and Cannas, Marco and Bauer, Sophie and Perisse, Jocelyn and Macé, Jean Reynald and Boscaino, Roberto and Boukenter, Aziz and Ouerdane, Youcef and Nacir, B. and Girard, Sylvain Neutron-induced defects in optical fibers. (2014) In: 10th International Symposium on SiO2 Advanced Dielectrics and Related Devices (SiO2014), 16 June 2014 - 18 June 2014 (Cagliari, Italy).

Any correspondence concerning this service should be sent to the repository administrator: tech-oatao@listes-diff.inp-toulouse.fr

Neutron-induced defects in optical fibers

S.Rizzolo[123a)], A. Morana[1], M. Cannas[2], S. Bauer[3], J. Perisse[4], J-R. Mace[5], R. Boscaino[2], A. Boukenter[1], Y. Ouerdane[1], B. Nacir[6], S. Girard[1]

[1] *Laboratoire Hubert Curien, Université Jean Monnet, CNRS UMR 5516, Saint-Etienne, France*
[2] *Dipartimento di Fisica e Chimica, Università di Palermo, Palermo, Italy*
[3] *Areva Centre Technique, Le Creusot, France*
[4] *Areva NP, Lyon, France*
[5] *Areva NP, Paris, France*
[6] *Centre National de l'Energie, des Sciences et des Techniques Nucléaires, Maamoura, Morocco*

serena.rizzolo@univ-st-etienne.fr

Abstract. We present a study on 0.8 MeV neutron-induced defects up to fluences of 10^{17} n/cm² in fluorine doped optical fibers by using electron paramagnetic resonance, optical absorption and confocal micro-luminescence techniques. Our results allow to address the microscopic mechanisms leading to the generation of Silica-related point-defects such as E', H(I), POR and NBOH Centers.

PACS Keywords: Absorption, EPR, neutrons irradiation, RIA, luminescence, optical fibers

INTRODUCTION

Silica based optical fibers have recently attracted much interest for their applications in the nuclear field, mainly as a medium for data transport and also as sensors of temperature, strain and irradiation dose levels. The vulnerability of fiber-based applications is currently being studied to evaluate their performances and lifetimes when exposed to radiative constraints associated with natural or artificial environments. Depending on the applications, various harsh environments have to be considered in terms of particle types, dose and dose rate. Compared to others devices, optical fibers have favorable characteristics such as immunity to electromagnetic field, small size, light weight and fast response. However, their use in harsh environments associated with ionizing radiation is negative for the optical performance due to the generation of point defects that introduce localized levels within the forbidden band gap thus causing radiation induced absorption (RIA). The radiation effects in silica have been, therefore, the object of intensive studies over the last decades [1].

For a given fiber, radiation induced attenuation depends on various extrinsic parameters such as dose, dose rate, nature of radiation, temperature. In harsh environment, where optical fibers are employed as distributed sensors for various parameters such as temperature, strain, pressure for civil nuclear applications, are present both γ-rays and neutrons; this work focuses on neutron irradiation effect on optical fibers in order to understand the competition between the different mechanisms involved in defect generation.

A combination of complementary spectroscopy techniques permits us to study optical fibers and to identify the defects induced by radiation. By coupling absorption, luminescence and electron paramagnetic resonance we are able to identify the microscopic structure of defects such as *E' center*, ≡Si·; *nonbrinding oxygen hole center (NBOHC)*, ≡Si−O·; *peroxy radical (POR)*, ≡Si−O−O·; and *H(I)*, O=Si−H [2] in term of concentration and distribution over a transverse fibers cross section or along the fibers diameter.

The understanding of generation mechanisms of these defects is relevant to improve the radiation resistance of optical fibers. Previous studies have shown that pure silica core (PSC) and F-doped fibers exhibit low RIA in the UV-Visible spectral domain for high irradiation doses [1]; they are, for this reason, of particular interest for the design of radiation hardened distributed fiber sensors for nuclear industry.

The purpose of this work is to study the defects induced by neutron exposure (fission spectrum) in fluorine doped fibers and their influence on fiber optical properties.

EXPERIMENTAL PROCEDURE

We investigated the radiation responses of step index Fluorine doped optical fibers. Fiber samples were designed starting from preforms fabricated by iXFiber-SAS for hardening studies with an experimental and simulative coupled approach. Radial distribution of fluorine amounts in studied fibers is reported in Figure 1; core's and cladding's diameters are of 42.5 µm and 125 µm, respectively, and the coating is in Acrylate.
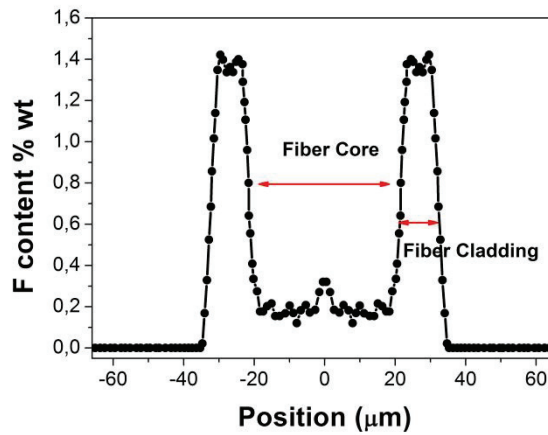

FIGURE 1: Fluorine contents as a function of the position along the diameter of the fiber in pristine sample.

The neutron irradiations were performed at the 2 MW pool-type TRIGA Mark II reactor of the CNESTEN, Centre National de l'Energie, des Sciences et des Techniques Nucléaires, (Maamoura, Morocco). The neutron flux is 2.1×10^{12} n/(cm^2·s) and the associated γ-dose-rate is 40 Gy/s; the accumulated fluence varies between 10^{15} n/cm^2 (with an additional γ-dose of 0.02 MGy) and 10^{17} n/cm^2 (with an additional γ-dose higher than 2 MGy).

RIA was measured with the well-known cutback method; we injected light from a Halogen source into the sample; the signal transmitted through the fiber link was analyzed with a UV-Visible optimized spectrometer from 200 to 900 nm.

Confocal micro luminescence (CML) measurements were performed on neutron irradiated samples to highlight the NBOHC distribution along the fibers diameter. All the measurements were recorded using an Aramis spectrometer associated with a He-Cd ion laser excitation line (energy 3.8 eV, power few µW) and supplied with a CCD camera, micro translation stages and a x40 objective. The employed experimental conditions lead to a spatial resolution of about 3µm.

EPR spectra were investigated in order to detect and quantify the paramagnetic defects in our silica samples. E'-Si and H(I) defects are probed at room temperature (300 K), whereas NBOH and POR centers were checked at low temperature (77K) using a Bruker EMX-Micro Bay spectrometer working at 9.8 GHz with a magnetic-field modulation frequency of 100 kHz. The defect concentrations were estimated using the EPR signal recorded in a bulk sample with a known concentration of E'centers.

RESULTS

In Figure 2 RIA spectra are shown. From these measurements at least two different contributions are present. We find an UV-absorption tail which increases with increasing energy and an absorption band centered at around 2 eV that is known to be due to NBOHC defects [3].We can observe that RIA increases with increasing of irradiation doses. The attenuation level is of 0.27dB/m in sample irradiated at 10^{15}n/cm², 0.88dB/m at the fluence of 10^{16}n/cm² and 6.28dB/m for 10^{17}n/cm².

We studied NBOH centers thanks to their luminescence signal in the red domain (~1.9 eV) with an adapted CML measurements. The results are reported in Figure 3 at different fluencies, as for the absorption, the intensity of the photoluminescence (PL) band increases with increasing irradiation doses.

This luminescence band is an excellent support for a cartography view (Figure 3b) along the diameter of the fiber which highlights the NBOHC concentration in both the core and in the cladding zones. We compared the normalized PL at 1.9 eV associated with NBOHC at the three irradiation fluences with the Fluorine contents as a function of the position. As a consequence, we clearly distinguish that NBOHC defects concentration is higher in the fiber core than in the cladding parts. This is linked to the fact that Fluorine reduces strained bonds, the most likely NBOHC precursors [4]. However, we note that the inhibition of NBOHC from Fluorine depends on the dose; as shown in Figure 3(b), in fact, we see that for the lowest dose NBOHCs are mainly concentrated in the core. For 10^{16}n/cm² and more for 10^{17}n/cm² the volume of the fiber in which these defects are concentrated increases and for the highest dose we have a considerable amount of defects also in the cladding.
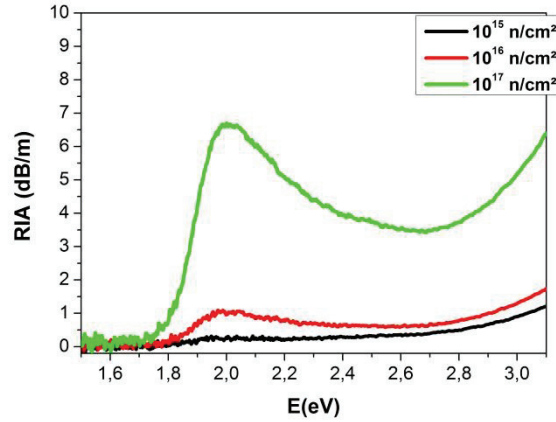

FIGURE 2: RIA spectra in UV-visible range for the samples irradiated at 10^{15} n/cm², 10^{16} n/cm² and 10^{17} n/cm².

In Table 1 we report the values for optical absorption (OA) at 2 eV and luminescence (PL) at 1.9 eV. We also correlated the PL with the absorption in order to establish whether the absorption band in our samples is due to the contribution of a single defect as discussed in [5].

TABLE 1: Evolution of optical absorption (OA at 2 eV) and luminescence (PL at 1.9 eV) with the fluence.

Fluence (n/cm²)	OA (dB/m) (2 eV)	PL (a.u.) (1.9 eV)
10^{15}	0.27±0.07	27±2
10^{16}	0.88±0.07	106±6
10^{17}	6.28±0.07	660±30

Considering the cartography in Figure 3(b) we can assume that the absorbing centers are located mainly in the fiber core giving rise to the RIA band reported in Figure 2. Moreover, from absorption, thanks to Smakula's equation, knowing the oscillator strength of NBOHC ($f=1.91 \cdot 10^{-4}$) [6], and the refractive index at 2eV ($n=1.46$) [7], we estimate the NBOHCs' concentration to be around $5.4 \cdot 10^{15} \mathrm{cm}^{-3}$ in sample irradiated at $10^{15} \mathrm{n/cm^2}$, $1.4 \cdot 10^{16} \mathrm{cm}^{-3}$ at the fluence of $10^{16} \mathrm{n/cm^2}$ and $10^{17} \mathrm{cm}^{-3}$ for $10^{17} \mathrm{n/cm^2}$.
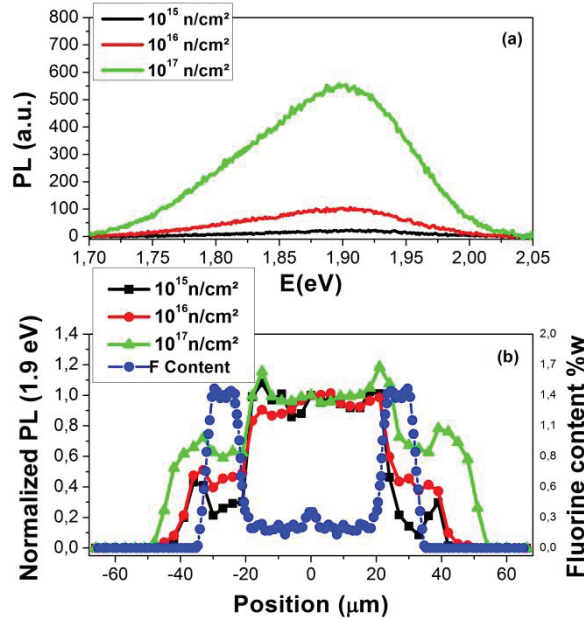

FIGURE 3: (a) PL spectra measured under excitation at $E_{exc}=3.8$ eV in the core center of neutron irradiated samples at 10^{15} n/cm², 10^{16} n/cm² and 10^{17} n/cm²; (b) NBOHC normalized profiles along the fiber diameter of the fibers (points black 10^{15} n/cm²; points red 10^{16} n/cm²; points green 10^{17} n/cm²) compared with Fluorine content along the diameter (points blue). The points have a spatial resolution of 3 μm.

The electron paramagnetic resonance was used to identify the paramagnetic centers present in the sample.

One of the most common paramagnetic intrinsic defects is the E' characterized by axial symmetry; its EPR spectrum is usually recorded at RT. A variant of the E' center can be also observed in EPR spectra, the H(I) defect, consisting of a dangling Si bond with one neighboring O substituted by a H atom. The hyperfine interaction between the unpaired electron and the H nucleus, with spin of 1/2, originates the doublet of 74 G. In contrast to these centers, the oxygen-related defect signals (NBOHC and POR) are large (~30 G) and they overlap, so they cannot be distinguished at RT; measurements at low temperature, 77 K (liquid nitrogen), are needed to separate the two contributions.

Figure 4 reports the studied paramagnetic defects induced in the neutron irradiated sample at the highest dose of 10^{17} n/cm²: in (a) the axial symmetry lineshape related to E' center; in (b) the hyperfine doublet at 74 G associated with H(I) defect and in (c) the overlap of NBOH and POR centers lineshapes, whose relative contribution could be estimated by a deconvolution.

The obtained EPR signal is proportional to the first derivative of the absorption line and the double integral of the EPR spectrum is proportional to the number of centers. So the absolute concentration of defects can be estimated by comparing the double integral of the EPR spectrum with a reference sample. For this aim, we used an irradiated silica bulk sample whose E' concentration was known by spin-echo measurements, the accuracy of the absolute concentration being estimated as 50% whereas the relative error among the different defect types is about 20%.
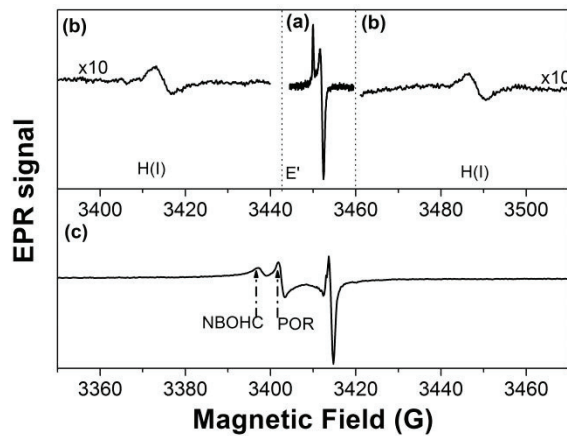
FIGURE 4: EPR first harmonic spectra in the samples irradiated at 10^{17} n/cm² normalized by the mass. The part (a) shows E' center line, in (b) is shown the doublet of the H(I) center, and the part (c) shows EPR spectrum associated with the NBOH and the POR centers.
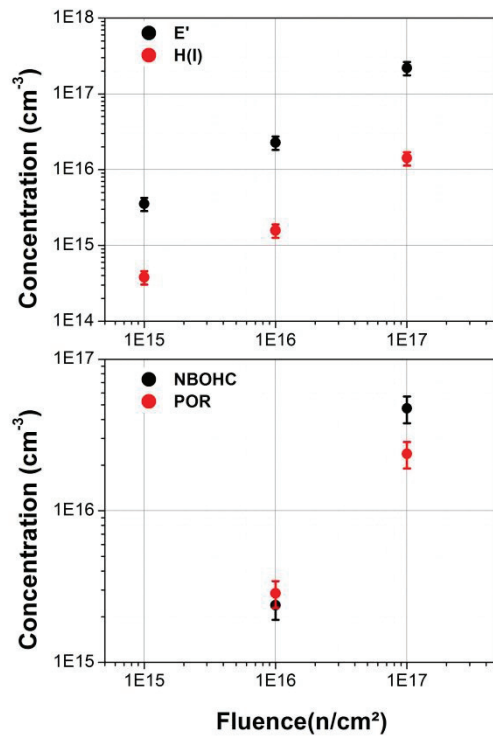

FIGURE 5: Concentration of (a) Si- E' (black points) and H(I) (red points) and (b) NBOHC (black points) and POR (red points) point defects as a function of neutron fluence.

The defect concentrations as a function of the neutron fluence are reported in Figure 5. All defect concentrations increase with the fluence, following an almost linear trend; E' center evidences the largest concentration.

For NBOHC, the evaluated concentration is of the same order of magnitude as the result calculated from absorption measurements. It is, indeed, shown from CML results that NBOHCs are more concentrated in the core of the fiber.

DISCUSSION

The above reported results are interpreted on the basis of the processes activated by neutrons in the silica network trying to understand the role of precursors and the reactions of induced defects with diffusing species such as H, O or their compounds. Neutron irradiation produces in the fiber intrinsic defects, as E', NBOHCs and PORs, whose concentration grows without saturating at the maximum neutron fluence of 10^{17}n/cm^2. It can be observed that in silica bulk, reported in literature, the concentration of the E' centers induced by irradiation is much higher than that of the oxygen related defects [8], because the main precursors are the impurities, whereas for the fibers the concentrations of the E', NBOHC and POR defects are of the same order of magnitude.

The presence of H(I) seems singular, as the samples are not hydrogenated and the H_2-concentration inside the fiber is low; it can be generated from H atoms that can come from the breakage of an O-H bond or from the acrylate coating from where hydrogen atoms are released and diffused in the fiber glass [9].

It is known that NBOHCs can be created by the radiolysis of ≡Si-OH bonds or the cleavage of strained ≡Si-O-Si≡ bonds [10]. Since the OH content is low in our fibers, the most likely precursors of NBOHCs are the strained bonds. However we know also that the fluorine hinders the generation of NBOHCs reducing the effective volume where NBOHCs are formed [4], as pointed out by the anticorrelation existing between the NBOHC concentration and the F content of Figure 3b.

The paramagnetic defect concentration exhibit a linear trend. The precursors come from the matrix glass that at these fluences can be considered as an infinitive bath.

In these conditions some possible mechanisms for defects generation can be suggested:

- breakage of strained bond that leads to formation of a couple E' and NBOH Centers:

$$\equiv Si \cdots O - Si \equiv \; \rightarrow \; \equiv Si \cdot + \equiv Si - O \cdot$$

- breakage of a peroxy linkage that give an E' and a POR :

$$\equiv Si - O - O - Si \equiv \; \rightarrow \; \equiv Si \cdot + \equiv Si - O - O \cdot$$

- a linkage of a free hydrogen atom and a twofold coordinated silicon leads to the formation of an H(I):

$$= Si \cdot\cdot + H \rightarrow = Si \cdot - H$$

CONCLUSION

Defects induced in Fluorine-doped multimode fiber by 0.8 MeV neutrons have been investigated by absorption, CML and EPR experiments. We generated and observed a radiation induced attenuation in the visible range that we attributed to NBOH centers, thanks to the correlation with luminescence band at 1.9eV. From comparison of these spectroscopical techniques we estimated the concentration of this defect and its distribution along the diameter of the fiber. Number of centers increases with increasing neutron fluence up to a maximum concentration of 10^{17}cm^{-3}. Moreover, we have evidenced paramagnetic defects related to the silica network, Si- E', H(I), NBOHC and POR, and their average concentration growth linearly with the neutron fluence. These results can be explained taking into account different mechanisms of defects generation that we summarize and which will be used to improve the radiation hardness of fiber sensors for the nuclear industry.

REFERENCES

1. S. Girard, J. Kuhnhenn, A. Gusarov, B. Brichard, M. Van Uffelen, Y. Ouerdane, A. Boukenter and C. Marcandella, "Radiation effects on silica-based optical fibers: recent advances and future challenges", IEEE Trans. Nucl. Sci., 60 (3), pp. 2015-2036 (2013).
2. L. Skuja, "Optically active oxygen-deficiency-related centers in amorphous silicon dioxide", J. Non-Cryst. Solids, 239, pp. 16-48 (1998).
3. A. Morana, M. Cannas, S. Girard, A. Boukenter, L. Vaccaro, J. Perisse, J-R Mace, Y. Ouerdane and R. Boscaino, "Origin of the visible absorption in radiation-resistant optical fibers", Opt. Mater. 3 (10), pp.1769-1776 (2013).
4. L. Vaccaro, M. Cannas, S. Girard, A. Alessi, A. Morana, A. Boukenter, Y. Ouerdane and R. Boscaino, "Influence of fluorine on the fiber resistance studied through the Non Bridging Oxygen Hole Center related luminescence", J. Appl. Phys., 113 (19), 193107 (2013).
5. M. Cannas, L. Vaccaro and B. Boizot, "Spectroscopic parameters related to non-bridging oxygen hole centers in amorphous-SiO2", J. Non-Cryst. Solids, 352, pp. 203-208 (2006).

6. L. Vaccaro, M. Cannas and R. Boscaino, "Phonon coupling of non-bridging oxygen hole center with the silica environment: Temperature dependence of the 1.9 eV emission spectra", J. Lumin., 128, pp. 1132-1136 (2008).
7. A.C. Wright, "Defect-free vitreous networks: the idealized structure of SiO2 and related glasses" in Defects in SiO2 and Related Dielectrics: Science and Technology, Editors: G. Pacchioni, L.Skuja e D.L. Griscom; Kluwer Academic Publishers; pp. 1-35 (2000).
8. J.C. Lagomacini, D. Bravo, M. Len, P. Martin, A. Ibarra, A. Martin and F.J. Lopez, "EPR study of gamma and neutron irradiation effects on KU1, KS-4V and Infrasil 301 silica glasses", J. Nucl. Mater., 417, pp. 802-805 (2011).
9. B. Brichard, P. Borgermans, A. Fernandez, K. Iammens and M. Decréton, "Radiation Effect in Silica Optical Fibers Exposed to Intense Mixed Neutron-Gamma Radiation Field," IEEE Trans. Nucl. Sci., vol. 48, no. 6, Dec. 1990.
10. L. Skuja, M. Hirano, H. Hosono and K. Kajihara, "Defects in oxide glasses", Phys. Status Solidi (c), 2 (1), pp. 15-24 (2005).